

**Supporting Information for**  
**Asymmetric Acceptors with Fluorinated and Chlorinated**  
**End-Groups Enabling Organic Solar Cells with Approaching**  
**19% Efficiency and High Thickness-Tolerance**

Dandan Li <sup>a†</sup>, Wenrong Zhao <sup>a†</sup>, Gang Li <sup>a\*†</sup>, Yan Xu <sup>a</sup>, Lin Da <sup>c</sup>, Ping Zhou <sup>d</sup>, Peng Yang <sup>a\*</sup> and Bo Tang <sup>a,b \*</sup>

*<sup>a</sup> College of Chemistry, Chemical Engineering and Materials Science, Key Laboratory of Molecular and Nano Probes, Ministry of Education, Collaborative Innovation Center of Functionalized Probes for Chemical Imaging in Universities of Shandong, Shandong Normal University, Jinan 250014, Shandong Province, P. R. China.*

*<sup>b</sup> Laoshan Laboratory, 168 Wenhai Middle Road, Aoshanwei Jimo, Qingdao 266237, Shandong.*

*<sup>c</sup> Shanghai Institute of Applied Physics, Chinese Academy of Sciences.*

*<sup>d</sup> Shanghai Advanced Research Institute, Chinese Academy of Sciences.*

\* Corresponding author, E-mail: [ligang@sdnu.edu.cn](mailto:ligang@sdnu.edu.cn); [yangpeng@sdnu.edu.cn](mailto:yangpeng@sdnu.edu.cn); [tangb@sdnu.edu.cn](mailto:tangb@sdnu.edu.cn)

## Materials and Methods

### Materials

**D18:** Poly[(2,6-(4,8-bis(5-(2-ethylhexyl-3-fluoro)thiophen-2-yl)-benzo[1,2-b:4,5-b']dithiophene))-alt-5,5'-(5,8-bis(4-(2-butyloctyl)thiophen-2-yl)dithieno[3',2':3,4;2'',3'':5,6]benzo[1,2-c][1,2,5]thiadiazole)]

**PM6:** Poly[(2,6-(4,8-bis(5-(2-ethylhexyl-3-fluoro)thiophen-2-yl)-benzo[1,2-b:4,5-b']dithiophene))-alt-(5,5'-(1',3'-di-2-thienyl-5',7'-bis(2-ethylhexyl)benzo[1',2'-c:4',5'-c']dithiophene-4,8-dione)]

**Y6:** 2,2'-((2Z,2'Z)-((12,13-bis(2-ethylhexyl)-3,9-diundecyl-12,13-dihydro-[1,2,5]thiadiazolo[3,4-e]thieno[2'',3'':4',5']thieno[2',3':4,5]pyrrolo[3,2-g]thieno[2',3':4,5]thieno[3,2-b]indole-2,10-diyl)bis(methanylylidene))bis(5,6-difluoro-3-oxo-2,3-dihydro-1H-indene-2,1-diylidene))dimalononitrile

**L8-BO:** 2,2'-((2Z,2'Z)-((12,13-bis(2-ethylhexyl)-3,9-(2-butyloctyl)-12,13-dihydro-[1,2,5]thiadiazolo[3,4-e]thieno[2'',3'':4',5']thieno[2',3':4,5]pyrrolo[3,2-g]thieno[2',3':4,5]thieno[3,2-b]indole-2,10-diyl)bis(methanylylidene))bis(5,6-difluoro-3-oxo-2,3-dihydro-1H-indene-2,1-diylidene))dimalononitrile

**PNDIT-F3N:** Poly[[2,7-bis(2-ethylhexyl)-1,2,3,6,7,8-hexahydro-1,3,6,8-tetraoxobenzo[lmn] [3,8]phenanthroline-4,9-diyl]-2,5-thiophenediyl[9,9-bis[3'((N,N-dimethyl)-N-ethylamino) propyl]-9H-fluorene-2,7-diyl]-2,5-thiophenediyl]

**IC-2F:** 2-(5,6-difluoro-3-oxo-2,3-dihydro-1H-inden-1-ylidene)malononitrile

**IC-2Cl:** 2-(5,6-dichloro-3-oxo-2,3-dihydro-1H-inden-1-ylidene)malononitrile

**PEDOT:PSS:** Poly(3,4-ethylenedioxythiophene)-poly(styrenesulfonate), aqueous solution (Heraeus Clevios P VP A 4083)

**FN:** 1-Fluoronaphthalene, 98%

**D18, PM6, Y6, L8-BO, PNDIT-F3N, IC-2F and IC-2Cl** were purchased from Solarmer Materials Inc. in Beijing. **PEDOT:PSS** was purchased from Heraeus. **FN** was purchased from Aladdin. Other chemicals and solvents are purchased from J&K, Aladdin, Innochem and Energy Chemical and used as received. Toluene and tetrahydrofuran (THF) were distilled from sodium benzophenone under nitrogen. Anhydrous DMF was distilled from  $\text{CaH}_2$  under nitrogen. All the reactions dealing with air- or moisture-sensitive compounds were carried out in a dry reaction vessel under a positive pressure of nitrogen and heated by metal sand bath (WATTCAS, LAB-500, <http://www.wattcas.com>).

## Instruments and Measurement

$^1\text{H}$  NMR spectra were recorded on a Bruker AVIII-400M (400 MHz and 100 MHz, respectively) spectrometer at room temperature. Chemical shifts ( $\delta$ ) are reported in ppm.  $^1\text{H}$  NMR chemical shifts were determined relative to internal standard  $\text{CDCl}_3$  ( $\delta$   $^1\text{H}$ , 7.26 ppm,  $^{13}\text{C}$ , 77.16 ppm).<sup>1</sup> The spectroscopic solvents were purchased from Cambridge Isotope Laboratories. The following abbreviations are used to explain the multiplicities: s = singlet, d = doublet, t = triplet, q = quartet, m = multiplet, br = broad. Analytical thin layer chromatography (TLC) was performed on 0.25 mm silica gel 60 F254 plates and viewed by UV light (254 nm). Column chromatographic purification

was performed using 100-200 or 200-300 mesh silica gel. Mass spectra were measured on a Bruker Maxis UHR-TOF MS spectrometer.

### **Solar cell fabrication and characterization**

**(i) Binary devices based on D18:L36 or D18:L37.** Solar cells were fabricated in a conventional device configuration of ITO/PEDOT: PSS/Active layer/ PNDIT-F3N/Ag. The ITO-coated glass substrates were cleaned by ultrasonic treatment in detergent, deionized water, acetone, and isopropyl alcohol under ultra-sonication for 15 minutes each and subsequently dried by a nitrogen blow. The glass substrates were treated by UV-Ozone for 15 min before use. PEDOT: PSS layer was spin-cast onto the ITO substrates at 4300 rpm for 30s. After baked at 150 °C for 20 minutes, the substrates were transferred into an argon-filled glove box. Then the D18:acceptor blends with 1:1.6 ratio were dissolved in chloroform with 1-Fluoronaphthalene (FN) as additive (the mixture is stirred at 100 °C for 1 hour in order to fully dissolve the solid and the concentration of D18 is set as 4 mg/mL.) After the films are fully dried, thermal annealing is performed at 100 °C for 10 minutes. After that, a methanol solution of PNDIT-F3N (0.5 mg mL<sup>-1</sup>) is spin-cast atop the active layer at 3000 rpm. A thin PNDIT-F3N layer (10 nm) and Ag layer (100 nm) were sequentially evaporated through a shadow mask under vacuum of  $1.5 \times 10^{-4}$  Pa.

**(ii) Ternary devices of PM6:Y6:L36.** Solar cells were fabricated in a conventional device configuration of ITO/PEDOT: PSS/Active layer/ PNDIT-F3N/Ag. The ITO-coated glass substrates were cleaned by ultrasonic treatment in detergent, deionized

water, acetone, and isopropyl alcohol under ultra-sonication for 15 minutes each and subsequently dried by a nitrogen blow. The glass substrates were treated by UV-Ozone for 15 min before use. PEDOT: PSS layer was spin-cast onto the ITO substrates at 4300 rpm for 30s. After baked at 150 °C for 20 minutes, the substrates were transferred into an argon-filled glove box. Then PM6:Y6:L36 blend with 1:0.8:0.4 ratio were dissolved in chloroform (the concentration of blend solutions are 13.2 mg/mL for all blend films). After the films are fully dried, thermal annealing is performed at 90 °C for 10 minutes. After that, a methanol solution of PNDIT-F3N ( $0.5 \text{ mg mL}^{-1}$ ) is spin-cast atop the active layer at 3000 rpm. The Ag layer (100 nm) was sequentially evaporated through a shadow mask under vacuum of  $1.5 \times 10^{-4} \text{ Pa}$ .

**(iii) Ternary devices of PM6:L8-BO:L36.** Solar cells were fabricated in a conventional device configuration of ITO/PEDOT: PSS/Active layer/ PNDIT-F3N/Ag. The ITO-coated glass substrates were cleaned by ultrasonic treatment in detergent, deionized water, acetone, and isopropyl alcohol under ultra-sonication for 15 minutes each and subsequently dried by a nitrogen blow. The glass substrates were treated by UV-Ozone for 15 min before use. PEDOT: PSS layer was spin-cast onto the ITO substrates at 4300 rpm for 30s. After baked at 150 °C for 20 minutes, the substrates were transferred into an argon-filled glove box. Then the PM6:L8-BO:L36 blends with 1:1.0:0.2 ratio were dissolved in chloroform (the concentration of blend solutions are 16.5 mg/mL for all blend films). After the films are fully dried, thermal annealing is performed at 100 °C for 10 minutes. After that, a methanol solution of PNDIT-F3N ( $0.5 \text{ mg mL}^{-1}$ ) is spin-cast atop the active layer at 3000 rpm. The Ag layer (100 nm) was

sequentially evaporated through a shadow mask under vacuum of  $1.5 \times 10^{-4}$  Pa.

#### **UV-visible (UV-Vis) absorption.**

UV-vis absorption spectra were performed with a Beijing Purkinje General Instrument Co. Ltd. TU-1901 spectrophotometer. All steady-state measurements were carried out using a quartz cuvette with a path length of 1 cm.

#### **Thermogravimetric (TGA) analysis.**

Thermogravimetric (TGA) analysis was carried out on a TA Instrument TA Q50 Thermogravimetric Analyzer at a heating rate of 10 °C/min up to 600 °C.

#### **Electrochemical Characterization.**

Cyclic voltammogram (CV) was performed with a CHI 660C electrochemical workstation at a scan rate of 100 mV/s. The highest occupied molecular orbital (HOMO) and lowest unoccupied molecular orbital (LUMO) energy levels were calculated from the onset oxidation potential and the onset reduction potential, using the equation  $E_{\text{LUMO}}/E_{\text{HOMO}} = -e (\phi_{\text{red}}/\phi_{\text{ox}} + 4.8 - \phi_{\text{Fc/Fc}^+})$  (eV), where  $\phi_{\text{Fc/Fc}^+}$  is the redox potential of ferrocene/ferrocenium (Fc/Fc<sup>+</sup>) couple in the electrochemical measurement system. The relevant energy level of Fc/Fc<sup>+</sup> was taken as 4.8 eV below vacuum.

#### **Space charge-limited current (SCLC) device fabrication**

The hole and electron mobility were measured using the space charge limited current

(SCLC) method, employing a diode configuration of ITO/PEDOT:PSS/active layer/MoO<sub>3</sub>/Ag for hole and glass/ITO/ZnO/active layer/ PNDIT-F3N /Al for electron by taking the dark current density in the range of 0-5 V and fitting the results to a space charge limited form, where SCLC is described by:

$$J = \frac{9\varepsilon_0\varepsilon_r\mu_0(V - V_{bi})^2}{8L^3}$$

where J is the current density, L is the film thickness of the active layer,  $\mu$  is the hole or electron mobility,  $\varepsilon_r$  is the relative dielectric constant of the transport medium,  $\varepsilon_0$  is the permittivity of free space ( $8.85 \times 10^{-12}$  F m<sup>-1</sup>), V is the applied voltage to the device and  $V_{bi}$  is the built-in voltage due to the relative work function difference of the two electrodes.

### **Atomic force microscope (AFM) Characterization**

AFM measurements were performed by using a Scanning Probe Microscope-Dimension 3100 in tapping mode. All film samples were spin-cast on glass/ITO substrates.

### **Grazing Incidence Wide angle X-ray Scattering (GIWAXS) Characterization**

The GIWAXS were conducted at Shanghai Synchrotron Radiation Facility (SSRF). All samples were prepared on ZnO-coated Si substrates using the same preparation conditions as for devices. All samples were irradiated at a fixed X-ray incident angle of 0.2° with an exposure time of 500s.

### **Transient photovoltage (TPV) and transient photocurrent (TPC) measurements.**

The instruments used in this test is TranPVC N900, Oriental Spectra. In TPV measurements, the devices were placed under background light bias enabled by a focused Quartz Tungsten-Halogen Lamp with an intensity of similar to working devices, *i.e.*, the device voltage matches the open-circuit voltage under solar illumination conditions. Photo-excitations were generated with an 8 ns pulses from a laser system (Oriental Spectra, NLD520). The wavelength for the excitation was tuned to 518 nm with a spectral width of 3 nm. A digital oscilloscope was used to acquire the TPV signal at the open-circuit condition. TPC signals were measured under short-circuit conditions under the same excitation wavelength without background light bias. The TPV and TPC decay curves were fitted with a single exponential function, and the decay constants were obtained from the fitting.

### **Energy loss.**

High sensitivity EQE and Electroluminescence quantum efficiency values were recorded with an electroluminescence measurement system (LST-EL, LightSky Technology Co., Ltd.) and  $V_{oc}$ -LOSS measurement system (VLAS, LightSky Technology Co., Ltd).

### **Theoretical calculations.**

Density functional theory (DFT) calculations were performed using the Gaussian 09 program with the B3LYP/6-31G(D,P) basis set. Calculations were performed in gas



phase without solvent effects. Vibrational frequency calculations were performed to check that the stable structures had no imaginary frequency.

## Supporting Figures

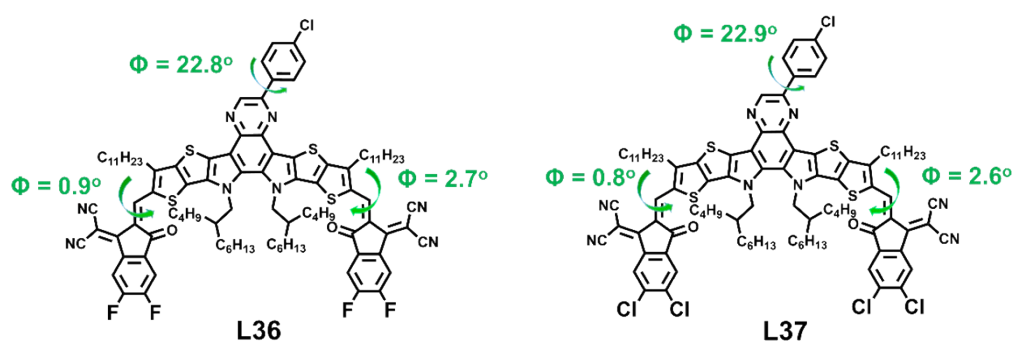


**Fig. S1.** The three dihedral angles of L36 and L37.

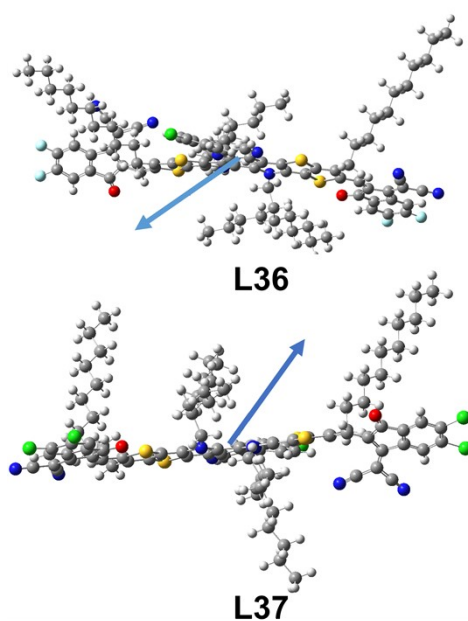


**Fig. S2.** Dipole moment direction of L36 and L37.

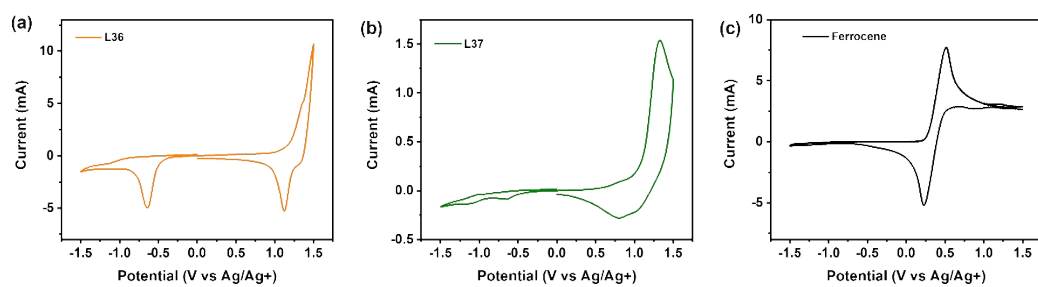


**Fig. S3.** Cyclic voltammetry measurements of (a) L36; (b) L37 and (c) Ferrocene measured in 0.1 M n-Bu<sub>4</sub>NPF<sub>6</sub> acetonitrile solution at a scan rate of 50 mV s<sup>-1</sup>.

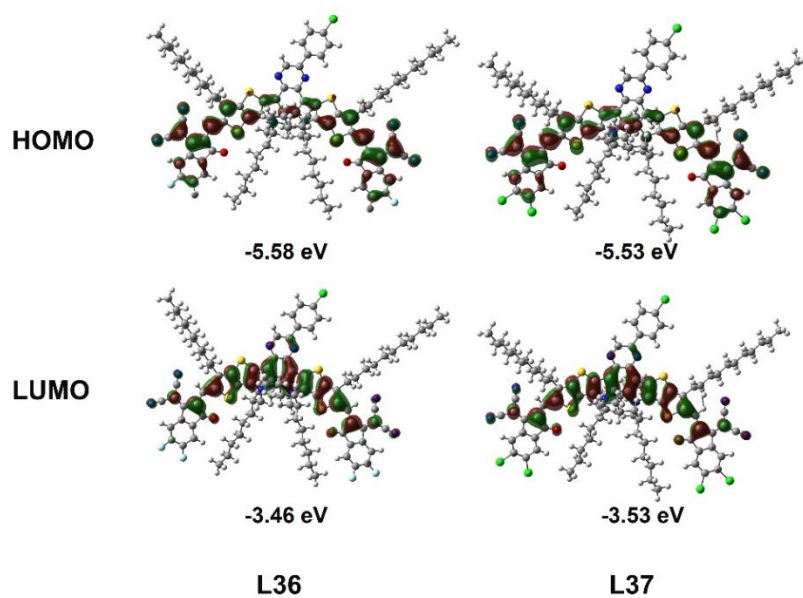


**Fig. S4.** The conformation and distribution of frontier molecular orbital for L36 and L37.

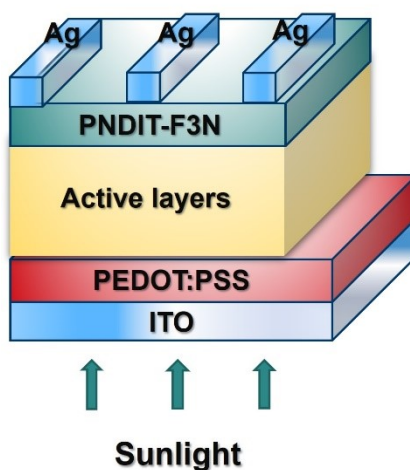


**Fig. S5.** The architecture of indium tin oxide (ITO)/poly(3,4-ethylenedioxythiophene)-poly(styrenesulfonate) (PEDOT:PSS)/active layers/poly-((2,7-bis(2-ethylhexyl)-1,2,3,6,7,8-hexahydro-1,3,6,8-tetraoxobenzo[*lmn*][3,8]phenanthroline-4,9-diyl)-2,5-thiophenediyl(9,9-bis(3-(dimethylamino)propyl)-9H-fluorene-2,7-diyl)-2,5-thiophenediyl) (PNDIT-F3N)/Ag.

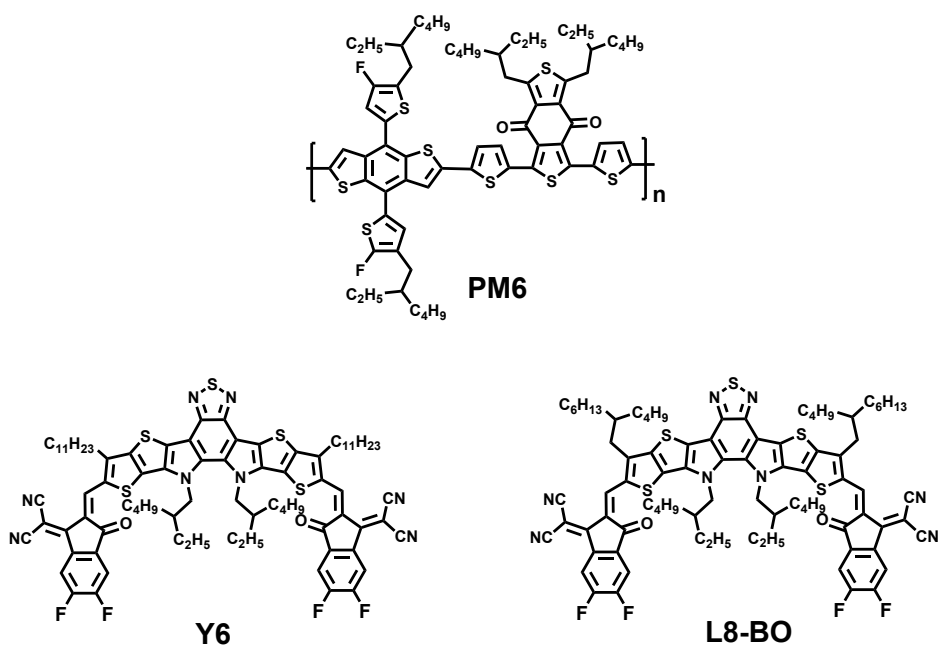


**Fig. S6.** The chemical structure of PM6, Y6 and L8-BO.

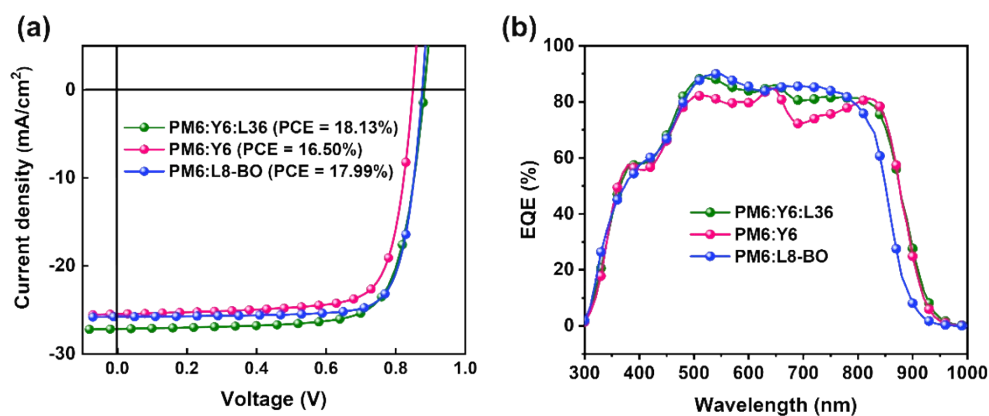


**Fig. S7.** (a)  $J$ - $V$  and (b) EQE characteristics of device based on PM6:Y6:L36, PM6:Y6 and PM6:L8-BO.

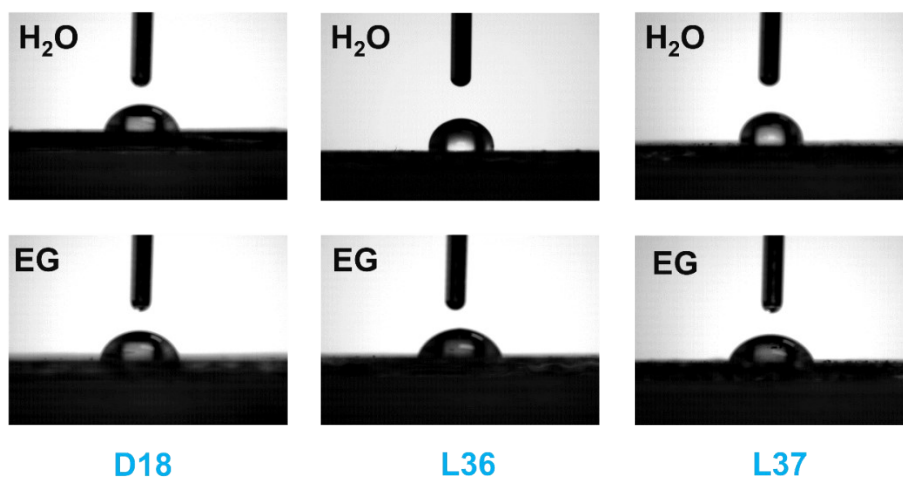


**Fig. S8.** Contact angle measurement images of the neat films of D18, L36 and L37 by using water and ethylene glycol (EG) liquid drops.

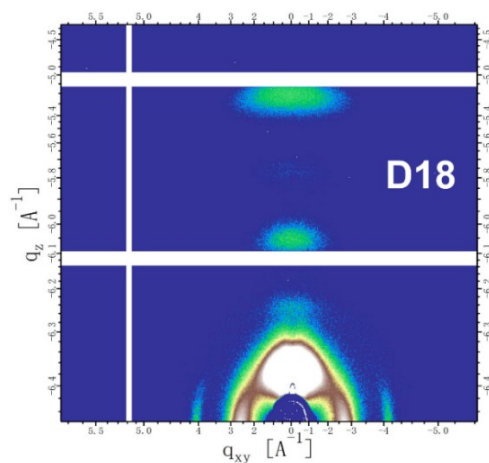


**Fig. S9.** The GIWAXS profile of donor D18.

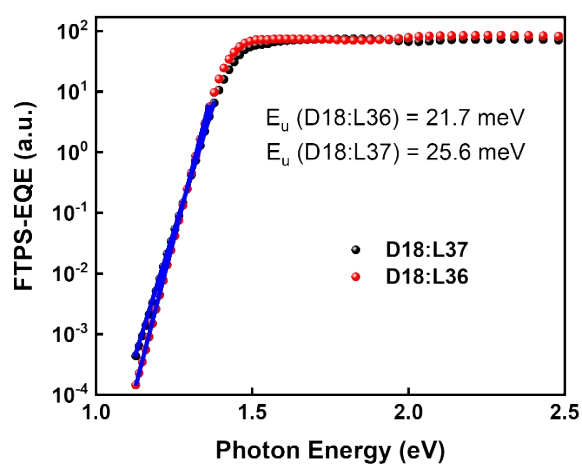


**Fig. S10.** Fitted curves of Urbach energy ( $E_u$ ) for binary devices.

## Supporting Tables

**Table S1.** Device optimization of PM6:L36 based binary system.

<i>D:A ratio</i>	<i>Volume</i>	<i>Post-treatment</i>	<i>V<sub>OC</sub> (V)</i>	<i>J<sub>SC</sub></i>	<i>FF</i>	<i>PCE</i>
<i>(m/m)</i>	<i>ratio of</i>			<i>(mA cm<sup>-2</sup>)</i>	<i>(%)</i>	<i>(%)</i>
	<i>FN</i>					

1:1.2	\	\	0.920	21.44	67.98	13.42
1:1.4	\	\	0.922	22.51	66.41	13.80
1:1.6	\	\	0.921	22.94	67.89	14.35
1:1.8	\	\	0.924	21.75	66.70	13.42
	0.1%	\	0.925	23.42	73.64	15.88
	0.2%	\	0.921	23.50	74.74	16.12
	0.3%	\	0.929	23.77	75.22	16.55
	0.4%	\	0.923	23.88	74.23	16.29
1:1.6		90 °C 5min	0.919	24.99	73.35	16.87
		100 °C 5min	0.920	24.93	74.67	17.06
	0.3%	110 °C 5min	0.917	25.33	72.62	16.78
		<b>100 °C 10min</b>	<b>0.901</b>	<b>25.84</b>	<b>75.82</b>	<b>17.74</b>
		100 °C 15min	0.899	25.33	75.37	17.24

**Table S2.** Charge mobilities of D18:L36 and D18:L37 measured by SCLC method.

<i>Sample</i>	<i>Hole mobility (<math>\mu_h</math>)</i>	<i>Electron mobility (<math>\mu_e</math>)</i>	$\mu_h/\mu_e$
D18:L36	$2.99 \times 10^{-4}$	$1.17 \times 10^{-4}$	2.55
D18:L37	$4.75 \times 10^{-4}$	$1.06 \times 10^{-4}$	4.48

**Table S3.** Key photovoltaic parameters calculated from the  $J_{ph}$ - $V_{eff}$  curves of D18:L36 and D18:L37 based devices.

<i>Sample</i>	$J_{sat}$ (mA cm <sup>-2</sup> )	$J_{ph}^b$ (mA cm <sup>-2</sup> )	$J_{ph}^c$ (mA cm <sup>-2</sup> )	$J_{ph}^b/J_{sat}$ (%)	$J_{ph}^c/J_{sat}$ (%)
D18:L36	26.31	25.43	21.64	96.66	82.25
D18:L37	23.02	21.61	17.73	93.87	77.02

<sup>a</sup>The  $J_{ph}$  under condition of  $V_{eff} = 1.0$  V; <sup>b</sup>The  $J_{ph}$  under short circuit condition; <sup>c</sup>The  $J_{ph}$  under maximum power output condition.

**Table S4.** Summary of contact angles ( $\theta$ ), surface tensions ( $\gamma$ ), and Flory-Huggins interaction parameters ( $\chi$ ) for various films.

<i>Surface</i>	$\theta_{water}(^\circ)$	$\theta_{EG}(^\circ)$	$\gamma$ (mN m <sup>-1</sup> )	$\chi^{D-A}$
D18	97.55	72.96	23.39	-
L36	96.41	68.75	27.54	0.170
L37	93.37	69.27	24.15	0.006

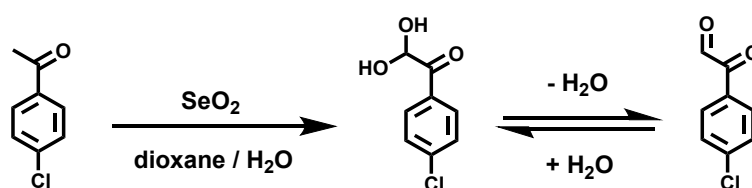
**Table S5.** Morphology data of donor and acceptor in the pristine and blend films.

Sample	(100) stacking, IP direction				(010) stacking, OOP direction			
	$q$ ( $\text{\AA}^{-1}$ )	$^a d$ ( $\text{\AA}$ )	FWHM	$^b \text{CCL}$	$q$ ( $\text{\AA}^{-1}$ )	$^a d$ ( $\text{\AA}$ )	FWHM	$^b \text{CCL}$
			( $\text{\AA}^{-1}$ )	( $\text{\AA}$ )			( $\text{\AA}^{-1}$ )	( $\text{\AA}$ )
L36	0.312	20.14	0.0755	79.42	1.760	3.57	0.217	25.94
L37	0.344	18.48	0.084	67.32	1.740	3.61	0.209	26.80
D18	0.310	20.27	0.0755	74.90	1.643	3.83	0.174	34.50
D18:L36	0.325	19.33	0.046	122.93	1.739	3.61	0.241	26.80
D18:L37	0.347	18.11	0.092	61.47	1.734	3.62	0.211	23.46

<sup>a</sup>Calculated from the equation:  $d\text{-spacing} = 2\pi/q$ . <sup>b</sup>Obtained from the Scherrer equation:  $\text{CCL} = 2\pi K/\text{FWHM}$ , where FWHM is the full-width at half-maximum and K is a shape factor ( $K = 0.9$ ).

## Synthetic details

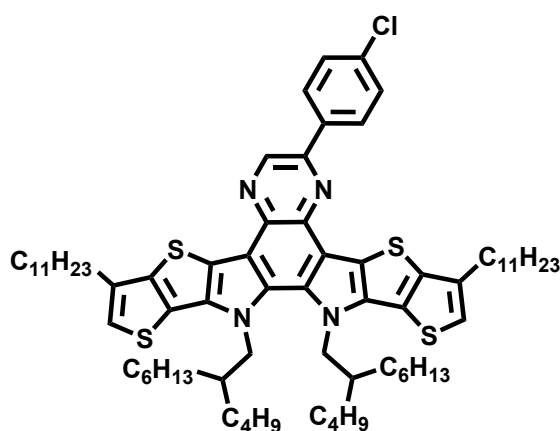
### Synthesis of compound 1-(4-chloro-phenyl)-2,2-dihydroxy-ethanone<sup>[2]</sup>





To a 100 ml three-neck flask was added selenium oxide (2.6 g, 23.4 mmol), dioxane (15 ml) and H<sub>2</sub>O (0.4 ml, 22.1 mmol), then heated to 105 °C until the solid was fully dissolved. Then 4-chloroacetophenone (2.0 g, 12.9 mmol) was added and the solution was refluxed with continued stirring for 6h. After the reaction mixture was cooled to room temperature and filtered with celite, the filtrate was extracted with dichloromethane three times. The combined organic layer was washed with water, dried over Na<sub>2</sub>SO<sub>4</sub>, and the solvents were distilled under reduced pressure. the residue was purified by column chromatography in THF /petroleum ether (1/4, v/v) to give the corresponding product as a light-yellow solid (1.54 g, 65% yield). <sup>1</sup>H NMR (400 MHz, CDCl<sub>3</sub>, chemical shifts are relative to the residue peak of CDCl<sub>3</sub> at 7.26 ppm): δ 8.07-8.05 (d, 2H), 7.47-7.45 (d, 2H), 6.31-6.29 (d, 1H), 5.01-4.98 (d, 1H).

*Synthesis of compound 13,14-bis(2-butyloctyl)-6-(4-chlorophenyl)-3,10-diundecyl-13,14-dihydrothieno[2'',3'':4',5']thieno[2',3':4,5]pyrrolo[3,2-f]thieno[2'',3'':4',5']thieno[2',3':4,5]pyrrolo[2,3-h]quinoxaline (2)*



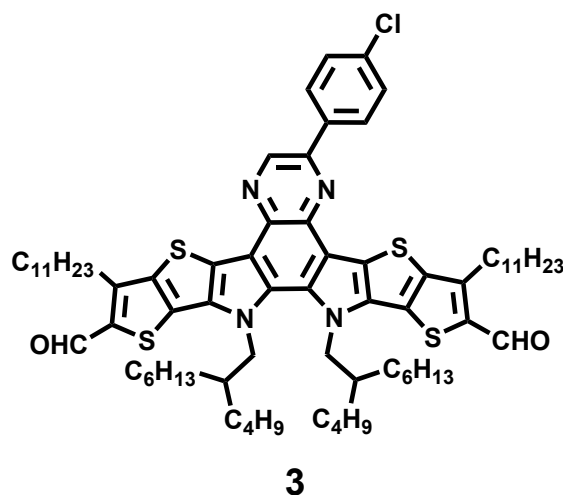
Compound 1 (300 mg, 0.28 mmol) was dissolved in 30 mL dry THF under an inert atmosphere and stirred about 20 mins under an ice-bath. Then lithium aluminum

hydride (213 mg, 5.6 mmol) was added partially by 4 times and stirred about 15 mins under the ice-bath. Next, the mixture was warmed up to 85 °C and stirred for 12 hours.

After cooling down to room temperature, cooled water was added dropwise to quench the remaining lithium aluminum hydride. The mixture was extracted with dichloromethane and the organic phase was dried with sodium sulfate. After the removal of the solvent, the crude product 1a was obtained and used immediately due to its instability under air.

To a 100 ml round bottom flask, the crude intermediate 1a (about 0.5 g) and 1-(4-chloro-phenyl)-2,2-dihydroxy-ethanone (209 mg, 1.12 mmol) were dissolved in pyridine (17 mL, analytical purity) under nitrogen. After being heated at 120 °C overnight, 50 ml dilute HCl was added. The aqueous phase was extracted with dichloromethane and the organic layer was washed with dilute HCl and dried over Na<sub>2</sub>SO<sub>4</sub>, filtered and purified with column chromatography on silica gel using dichloromethane /petroleum ether (1/10, v/v) as the eluent to give a red viscous liquid **2** (265 mg, 80% yield). <sup>1</sup>H NMR (400 MHz, CDCl<sub>3</sub>, chemical shifts are relative to the residue peak of CDCl<sub>3</sub> at 7.26 ppm): δ 9.42 (s, 1H), 8.39-8.37 (d, 2H), 7.62-7.60 (d, 2H), 7.02 (s, 2H), 4.66-4.65 (d, 4H), 2.86 (s, 4H), 2.18-2.09 (br, 2H), 2.07-1.81 (br, 6H), 1.74-1.58 (br, 4H), 1.49-1.18 (m, 38H), 1.15-0.66 (m, 32H), 0.65-0.55 (m, 6H).

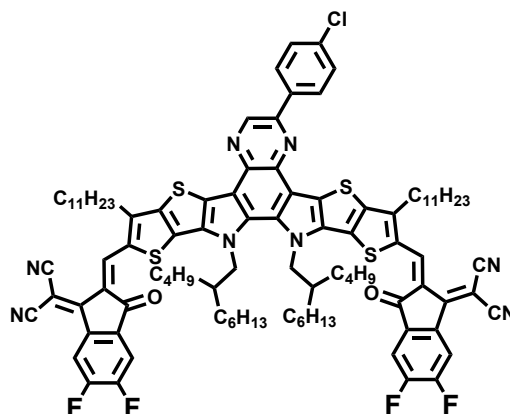
Synthesis of compound 13,14-bis(2-butyloctyl)-6-(4-chlorophenyl)-3,10-diundecyl-13,14-dihydrothieno[2'',3'':4',5']thieno[2',3':4,5]pyrrolo[3,2-f]thieno[2'',3'':4',5']thieno[2',3':4,5]pyrrolo[2,3-h]quinoxaline-2,11-dicarbaldehyde (3)



Under nitrogen protection, dry DMF (0.63 mL, 8.17 mmol) was cooled at 0 °C, then phosphorous oxychloride (0.20 mL, 2.18 mmol) was added slowly, and stirred at 0 °C for 2 h. Next, compound 2 (265 mg, 0.22 mmol) dissolved in dry dichloroethane (13 mL) and added dropwise to the DMF-POCl<sub>3</sub> solution. Then the solution was stirred for 12 h at 90 °C. The reaction mixture was poured into sodium acetate aqueous solution (150 mL) and then extracted with dichloromethane three times. The combined organic layer was washed with water, dried over Na<sub>2</sub>SO<sub>4</sub>, and the solvents were distilled under reduced pressure. the residue was purified by column chromatography in dichloromethane /petroleum ether (1/1, v/v) to give the corresponding product 3 as an orange viscous liquid (254 mg, 93% yield). <sup>1</sup>H NMR (400 MHz, CDCl<sub>3</sub>, chemical shifts are relative to the residue peak of CDCl<sub>3</sub> at 7.26 ppm): δ 10.16 (s, 1H), 10.15 (s, 1H), 9.44 (s, 1H), 8.37 (s, 1H), 8.35(s, 1H), 7.65 (s, 1H), 7.63 (s, 1H), 4.69-4.68 (d, 4H),

3.28-3.20 (m, 4H), 2.11 (br, 2H), 1.96 (br, 6H), 1.40-1.19 (m, 36H), 1.16-0.76 (m, 35H), 0.66-0.61 (m, 9H).

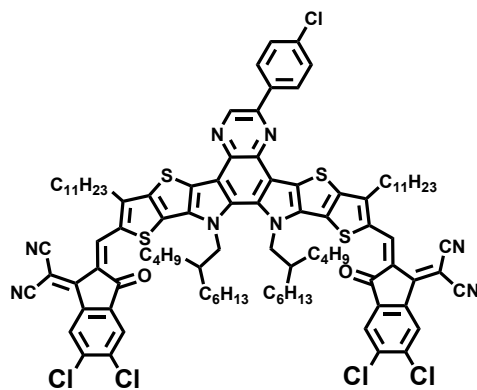
*Synthesis of compound 2,2'-((2Z,2'Z)-((13,14-bis(2-butyloctyl)-6-(4-chlorophenyl)-3,10-diundecyl-13,14-dihydrothieno[2'',3'':4',5']thieno[2',3':4,5]pyrrolo[3,2-f]thieno[2'',3'':4',5']thieno[2',3':4,5]pyrrolo[2,3-h]quinoxaline-2,11-diyl)bis(methaneylylidene))bis(5,6-difluoro-3-oxo-2,3-dihydro-1H-indene-2,1-diylidene))dimalononitrile (L36)<sup>[3]</sup>*



To a 50 ml round bottom flask, compound **3** (85 mg, 0.068 mmol), 5,6-difluoro-1,1-dicyanomethylene-3-indanone (IC-2F) (32 mg, 0.136 mmol), toluene (5 ml), acetic anhydride (0.1 ml) and boron trifluoride-ether complex (0.2 ml) were added under argon protection and stirred for 25 mins. After removal of organic solvent under reduced pressure, 50 ml methanol added and the precipitate was collected by filtration. The residue was purified by column chromatography on silica gel using a mixture solvent as eluent (dichloromethane/ petroleum ether, v/v = 1/1) to give L36 as a dark

solid (111 mg, 98% yield). <sup>1</sup>H NMR (400 MHz, CDCl<sub>3</sub>, chemical shifts are relative to the residue peak of CDCl<sub>3</sub> at 7.26 ppm): δ = 9.41 (s, 1H), 9.17 (d, 2H), 8.56 (t, 2H), 8.34 (d, 2H), 7.64 (d, 2H), 4.82 (br, 4H), 3.31-3.23 (m, 4H), 2.21 (br, 2H), 1.90-1.88 (m, 4H), 1.37-1.18 (br, 38H), 1.14-0.80 (br, 35H), 0.70-0.59 (m, 12H). <sup>13</sup>C NMR (101 MHz, CDCl<sub>3</sub>, chemical shifts are relative to the central peak of CDCl<sub>3</sub> at 77.16 ppm): δ = 186.30, 186.25, 158.76, 155.67, 154.19, 154.08, 153.23, 148.45, 146.46, 146.27, 139.87, 138.43, 138.40, 136.78, 136.55, 136.34, 136.23, 135.90, 135.38, 135.23, 134.59, 133.44, 133.35, 133.31, 133.18, 130.70, 130.44, 129.63, 128.40, 119.84, 119.75, 115.11, 114.92, 114.67, 112.61, 68.47, 55.88, 39.42, 32.06, 32.04, 31.77, 31.75, 31.61, 31.47, 30.60, 30.02, 29.88, 29.81, 29.78, 29.68, 29.48, 28.21, 28.11, 25.71, 25.61, 23.07, 22.82, 22.80, 22.65, 14.24, 14.22, 14.16, 13.96. **MALDI-TOF(m/z)**: calcd for C<sub>98</sub>H<sub>107</sub>Cl<sub>4</sub>N<sub>8</sub>O<sub>2</sub>S<sub>4</sub>: 1667.70580. found, 1667.70580.

*Synthesis of compound 2,2'-((2Z,2'Z)-((13,14-bis(2-butyloctyl)-6-(4-chlorophenyl)-3,10-diundecyl-13,14-dihydrothieno[2'',3'':4',5']thieno[2',3':4,5]pyrrolo[3,2-f]thieno[2'',3'':4',5']thieno[2',3':4,5]pyrrolo[2,3-h]quinoxaline-2,11-diyl)bis(methaneylylidene))bis(5,6-dichloro-3-oxo-2,3-dihydro-1H-indene-2,1-diylidene))dimalononitrile (L37)<sup>[3]</sup>*



To a 50 ml round bottom flask, compound 3 (85 mg, 0.068 mmol), 5,6-difluoro-1,1-dicyanomethylene-3-indanone (IC-2Cl) (36 mg, 0.136 mmol), toluene (5 ml), acetic anhydride (0.1 ml) and boron trifluoride-ether complex (0.2 ml) were added under argon protection and stirred for 25 mins. After removal of organic solvent under reduced pressure, 50 ml methanol added and the precipitate was collected by filtration. The residue was purified by column chromatography on silica gel using a mixture solvent as eluent (dichloromethane/ petroleum ether, v/v = 3/1) to give L37 as a dark solid (80 mg, 68% yield).  $^1\text{H}$  NMR (400 MHz,  $\text{CDCl}_3$ , chemical shifts are relative to the residue peak of  $\text{CDCl}_3$  at 7.26 ppm):  $\delta$  9.38 (s, 1H), 9.15 (d, 2H), 8.75 (d, 2H), 8.31 (d, 2H), 7.96 (s, 2H), 7.63 (d, 2H), 4.83 (br, 4H), 3.29-3.21 (m, 4H), 2.23 (br, 2H), 1.89-1.87 (m, 4H), 1.62-1.45 (br, 16H), 1.43-0.90 (m, 49H), 0.89-0.73 (m, 8H), 0.71-0.57 (m, 9H).  $^{13}\text{C}$  NMR spectrum of L37 was not obtained due to the limited solubility in  $\text{CDCl}_3$ . **MALDI-TOF**: calcd for  $\text{C}_{98}\text{H}_{107}\text{Cl}_5\text{N}_8\text{O}_2\text{S}_4$ : 1733.58465. found, 1733.58703.

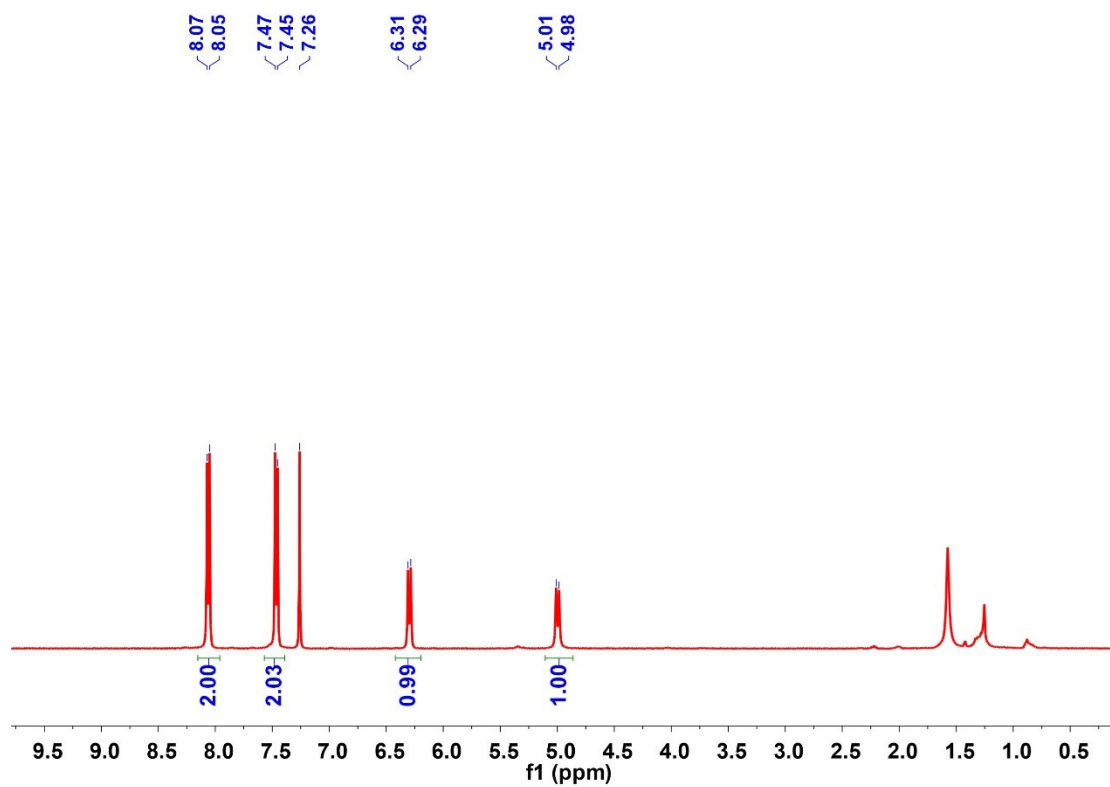


**Fig. S9.** <sup>1</sup>H NMR spectrum of compound 1-(4-chloro-phenyl)-2,2-dihydroxy-ethanone at 300K in CDCl<sub>3</sub>.

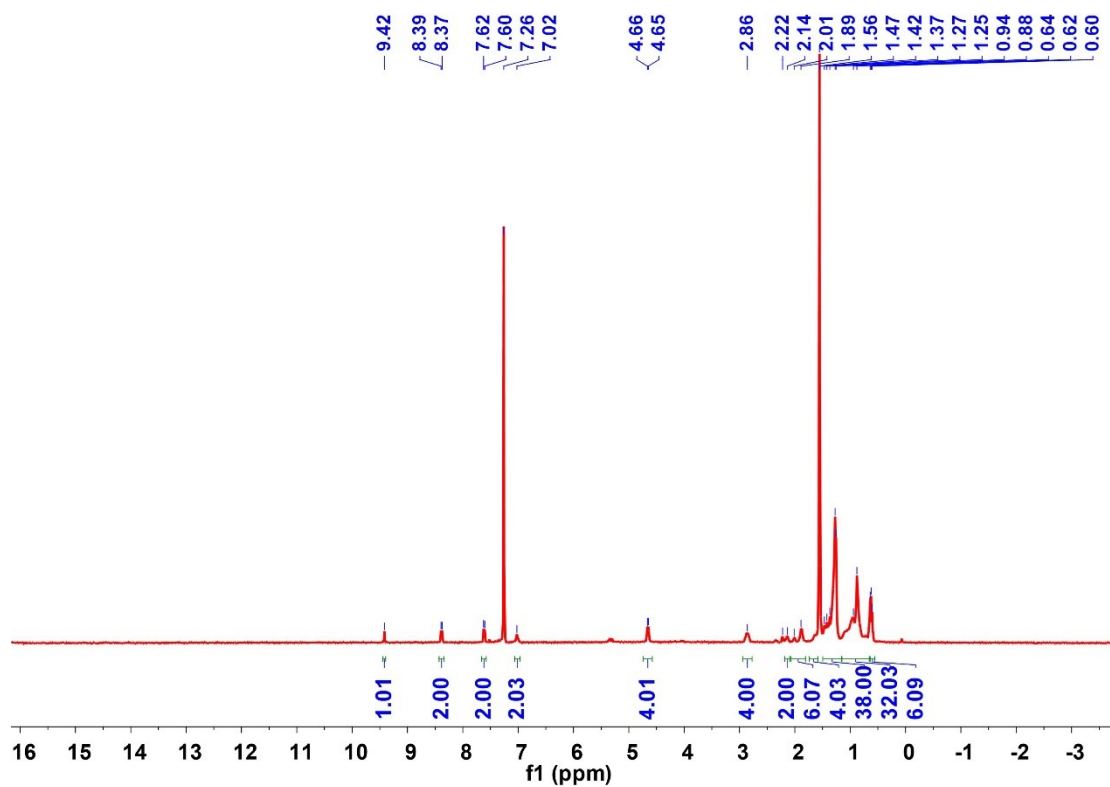


**Fig. S10.**  $^1\text{H}$  NMR spectrum of compound 2 at 300K in  $\text{CDCl}_3$ .

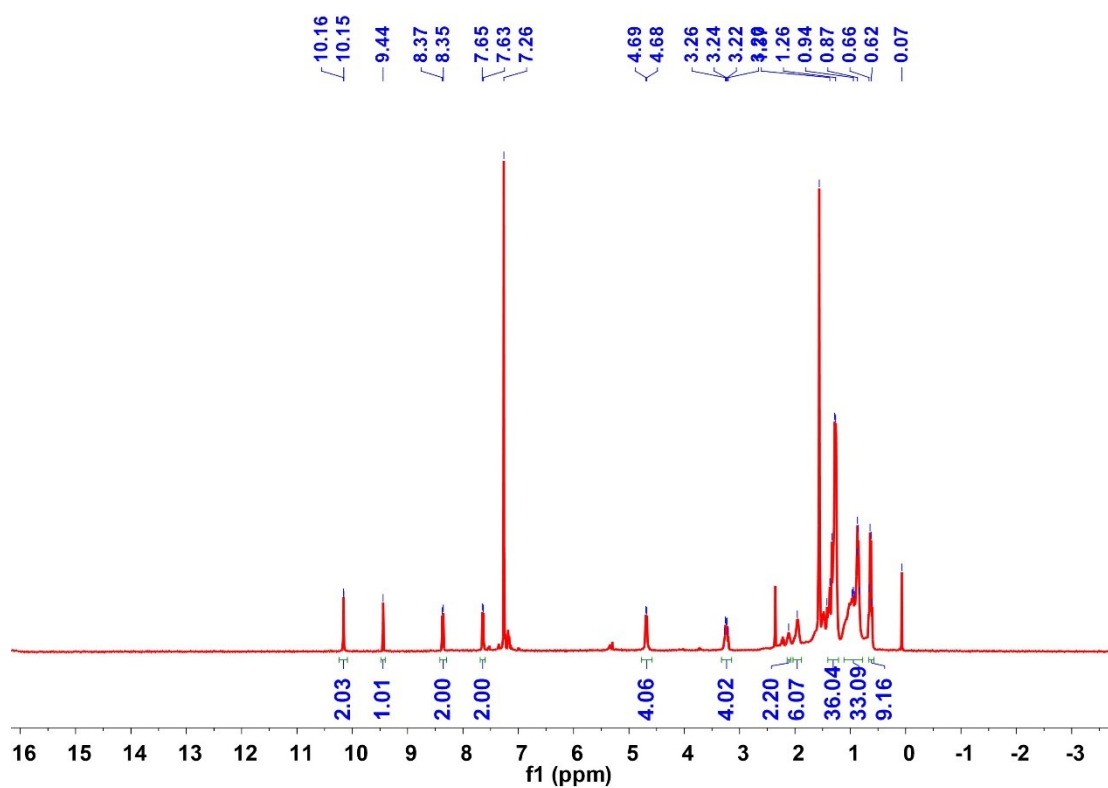


**Fig. S11.**  $^1\text{H}$  NMR spectrum of compound 3 at 300K in  $\text{CDCl}_3$ .



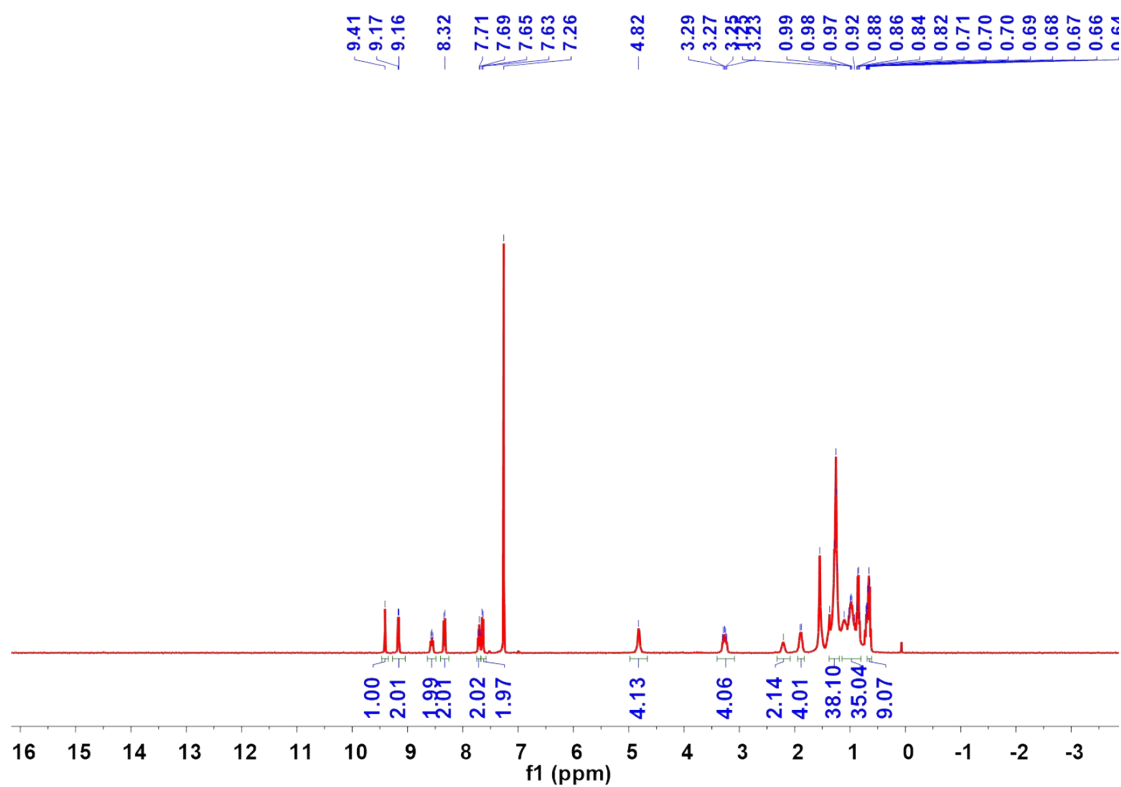


**Fig. S12.** <sup>1</sup>H NMR spectrum of compound L36 at 300K in CDCl<sub>3</sub>.

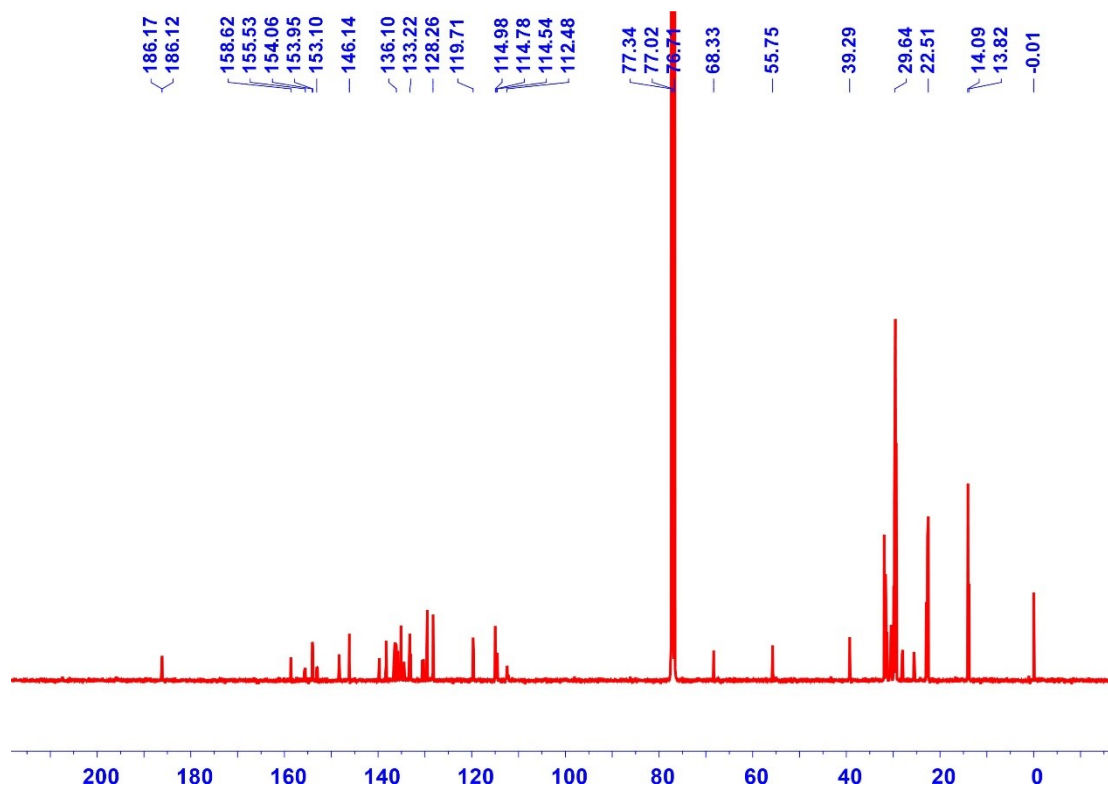


**Fig. S13.** <sup>13</sup>C NMR spectrum of compound L36 at 300K in CDCl<sub>3</sub>.

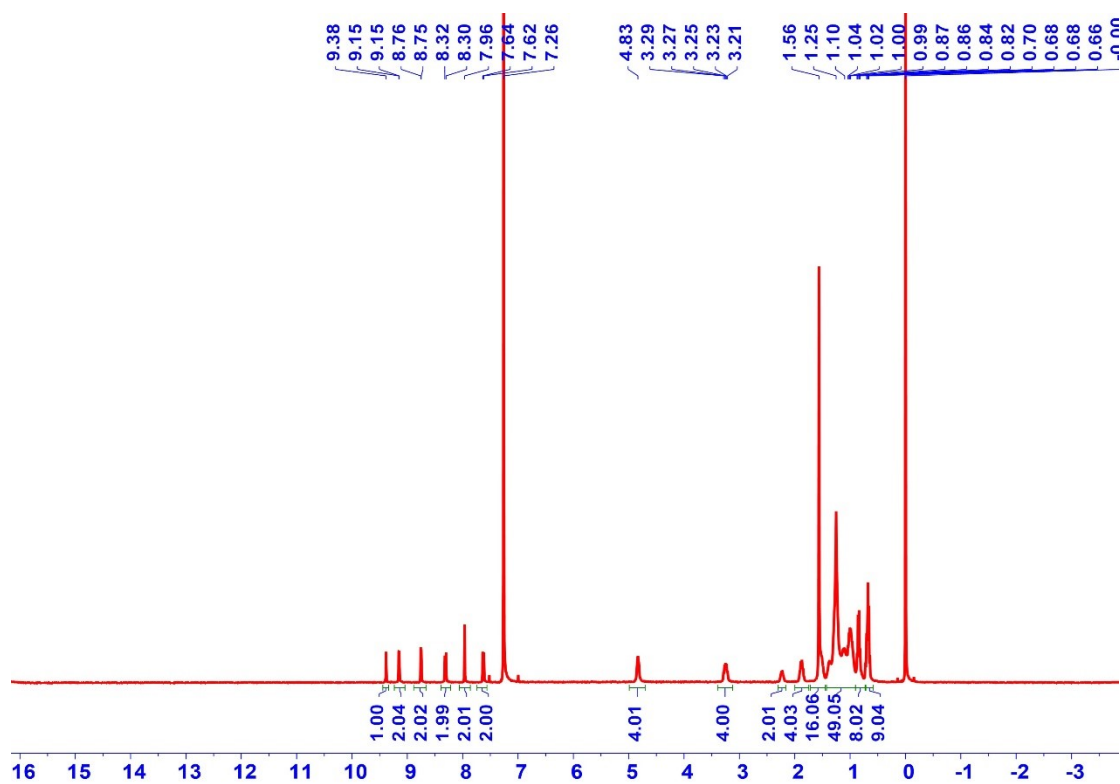


**Fig. S14.** <sup>1</sup>H NMR spectrum of compound L37 at 300K in CDCl<sub>3</sub>.

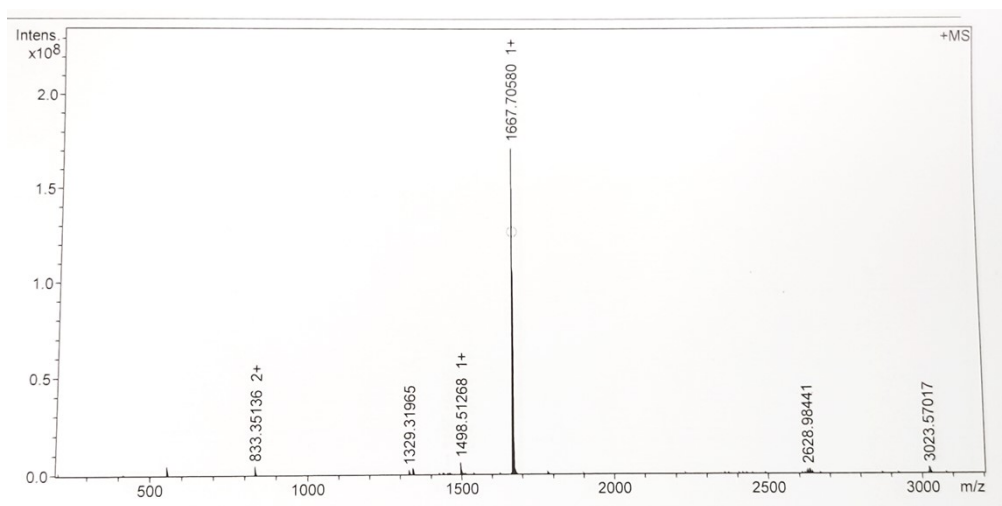


**Fig. S15.** MALDI-TOF mass spectrum of L36.

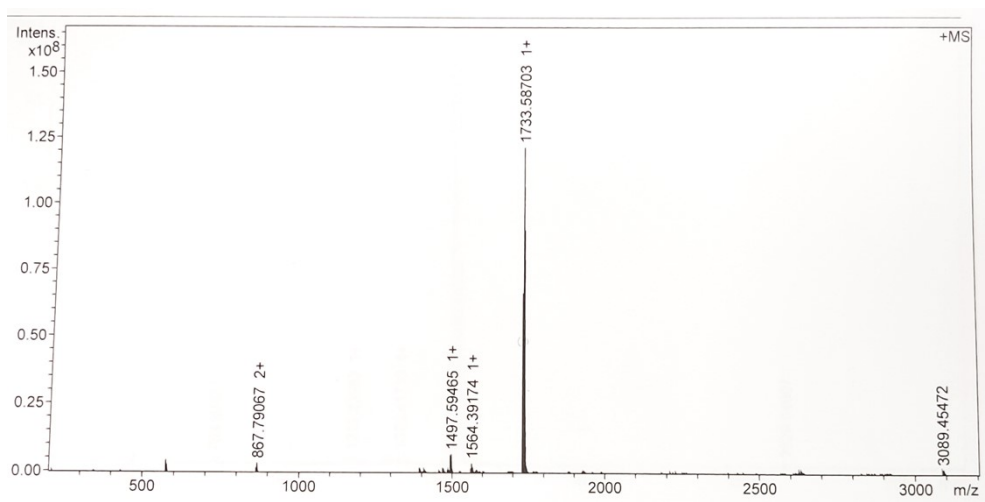


**Fig. S16.** MALDI-TOF mass spectrum of L37.

## Reference

1. H. E. Gottlieb, V. Kotlyar, A. Nudelman, *J. Org. Chem.* **1997**, *62*, 7512-7515.
2. P. Wang, W.-J. Tao, X.-L. Sun, S. Liao, Y. Tang, *J. Am. Chem. Soc.* **2013**, *135*, 16849-16852.
3. H. Fu, J. Yao, M. Zhang, L. Xue, Q. Zhou, S. Li, M. Lei, L. Meng, Z.-G. Zhang, Y. Li, *Nat. Commun.* **2022**, *13*, 3687.